The Astrophysical Journal, 628:474–477, 2005 July 20

LOW-ORDER ABERRATION SENSITIVITY OF EIGHTH-ORDER CORONAGRAPH MASKS

Stuart B. Shaklan and Joseph J. Green
Jet Propulsion Laboratory, California Institute of Technology, 4800 Oak Grove Drive, Pasadena, CA 91109;
stuart.shaklan@jpl.nasa.gov, joseph.j.green@jpl.nasa.gov
Received 2004 December 6; accepted 2005 February 23

ABSTRACT

In a recent paper, Kuchner, Crepp, and Ge describe new image-plane coronagraph mask designs that reject to eighth order the leakage of starlight caused by image motion at the mask, resulting in a substantial relaxation of image centroiding requirements compared to previous fourth-order and second-order masks. They also suggest that the new masks are effective at rejecting leakage caused by low-order aberrations (e.g., focus, coma, and astigmatism). In this paper, we derive the sensitivity of eighth-order masks to aberrations of any order and provide simulations of coronagraph behavior in the presence of optical aberrations. We find that the masks leak light as the fourth power of focus, astigmatism, coma, and trefoil. This has tremendous performance advantages for the *Terrestrial Planet Finder Coronagraph*.

Subject heading: astrobiology — planetary systems — techniques: high angular resolution

1. INTRODUCTION

The *Terrestrial Planet Finder Coronagraph* (*TPF-C*) is an optical, space-based telescope scheduled to fly in the next decade. It is designed to greatly reduce scattered light from a target star, enabling the direct detection of extrasolar terrestrial planets in reflected visible light as close as 62 mas from the star. Ford et al. (2004) review the mission and technical concepts.

The *TPF-C* coronagraph is designed to provide better than 1×10^{-10} rejection of starlight and 2.5×10^{-11} stability of the rejected starlight at angles larger than $4\lambda/D$, where λ is the wavelength (e.g., 550 nm) and D is the long dimension of the 8×3.5 m elliptical primary mirror. This is a very aggressive design; working so close to the center of the image plane presents many difficulties, the most significant being the high sensitivity of the scattered light level to changes in low-order aberration content. Green & Shaklan (2003) explored the sensitivity of various Lyot-type coronagraph designs to low-order aberrations.

Several coronagraph designs are being studied for *TPF-C* and other coronagraphic instruments, e.g., shaped pupil masks (Kasdin et al. 2003; Green et al. 2004), pupil remapping (Guyon 2003), four-quadrant phase masks (Rouan et al. 2003), and a shearing nulling interferometer (Shao et al. 2004). The coronagraph form that has so far demonstrated the best rejection of starlight is the band-limited mask (Kuchner & Traub 2002). Band-limited masks afford high extinction of diffracted light with ~30%–60% throughput and small inner working angles. A linear sinc^2 mask has been used in the *TPF* High Contrast Imaging Testbed (HCIT) to achieve $\sim 1 \times 10^{-9}$ rejection of light from a point source at $4\lambda/D$ (Trauger et al. 2004). So-called notch filter masks (Kuchner & Spergel 2003) are binary versions of the band-limited design that are manufactured using modern lithography techniques. Notch filter masks were first demonstrated by Debes et al. (2004) and are now under test in HCIT.

With the goal of reducing the sensitivity of image-plane masks to telescope pointing errors, Kuchner et al. (2005; hereafter KCG05) flattened and broadened the central lobe of the original band-limited mask by balancing the central curvature with an additional band-limited function. KCG05 called the new design an "eighth-order mask" because it rejects starlight leakage caused by a pointing error e as e^8. The approach is analogous to the flattening of the central lobe of a nulling interferometer through the interference of multiple beam pairs (Woolf & Angel 1997).

KCG05 state, "The order of the null dictates the sensitivity of the mask to optical aberrations." In this paper, we quantify this statement and show that eighth-order masks greatly reduce sensitivity to the following aberrations: focus, astigmatism, coma, and trefoil. To a lesser extent they also reduce sensitivity to spherical aberration and higher order aberrations.

We derive the aberration sensitivity in § 2. We then present modeling results and compare the performance of fourth-order and eighth-order masks in § 3. Some important implications for *TPF* are discussed in § 4.

2. ABERRATION SENSITIVITY

Adopting the notation of KCG05, the amplitude transmission function in the image plane for a linear (one-dimensional) mask is $\hat{M}(x)$. The mask transmission function is positive real, with $0 \leq \hat{M}(x) \leq 1$. The corresponding intensity transmission is $|\hat{M}(x)|^2$. We expand the amplitude transmission function in a Taylor series about the origin:

$$\hat{M}(x) = m_0 + m_1 x + m_2 x^2 + m_3 x^3 . \ldots \quad (1)$$

Let us consider the case in which the mask is opaque at the origin and symmetric, thus $m_0,\ m_1,\ m_3,\ m_5, \ldots = 0$. All the band-limited masks are designed so that their low spatial frequency parts can be described this way, although notch filter masks, like binary masks and sampled masks, aim to achieve the same effect with the addition of high spatial frequency components that might violate this rule (Kuchner & Spergel 2003). The eighth-order masks of KCG05 are designed to eliminate the quadratic term through the requirement

$$\left.\frac{\partial^2}{\partial x^2}\hat{M}(x)\right|_{x=0} = 0, \quad (2)$$

which in turn requires $m_2 = 0$. We are thus left with

$$\hat{M}(x) = m_4 x^4 + m_6 x^6 + m_8 x^8 . \ldots \quad (3)$$

Now consider light in the coronagraph pupil with amplitude transmission function $P(u)$ and phase transmission function $\phi(u) \ll 1$. The complex field at the pupil of radius r is then described by

$$E(u) = P(u)\exp^{i\phi(u)} = P(u)\left[1 + \sum_{l=1,2,3\ldots} \frac{i^l}{l!}\phi^l(u)\right], \quad (4)$$

where $P(u) = 1$ inside the pupil and 0 outside the pupil.

The instrument optics form an image at the coronagraph mask whose field is given by the Fourier transform of $E(u)$, $\hat{E}(x) = \mathrm{FT}(E(u))$. The field is then multiplied by $\hat{M}(x)$ to yield

$$\hat{F}(x) = \left(m_4 x^4 + m_6 x^6 + m_8 x^8 \ldots\right)\hat{E}(x). \quad (5)$$

Additional optics then form an image conjugate to the pupil plane where the field is expressed as the convolution of $E(u)$ with the Fourier transform of the mask (Gaskill 1978, p. 202),

$$F(u) = M(u) * E(u) = \sum_{k=4,6,8\ldots} m_k \left(\frac{-1}{i2\pi}\right)^k \frac{\partial^k}{\partial u^k} P(u)\left[1 + \sum_{l=1,2,3\ldots} \frac{i^l}{l!}\phi^l(u)\right]. \quad (6)$$

The field at the reimaged pupil is multiplied by a Lyot stop designed to block the light from an ideal wave front (the unity term of the expansion in eq. [4]). Band-limited masks achieve total rejection of unaberrated light inside the Lyot plane (Kuchner & Traub 2002). Thus, we can ignore edge effects in equation (6). The validity of this statement is borne out by computer simulations described in § 3.

Consider now the first term ($k = 4$, $l = 1$) of equation (6). This term is the fourth derivative of the wave front phase aberration[1] and vanishes for any aberration whose x-coordinate dependence is less than fourth order. For Noll-ordered Zernike aberrations (Noll 1976), the x-coordinate is third order or weaker for aberrations Z_j with $j = 2$–10 (see the Appendix).

To see the leakage due to tip-tilt ($\phi = a_2 Z_2 + a_3 Z_3$), we require $l = 4$, the ϕ^4 term of the wave front expansion. We then have $F(u) \propto a_2^4/4!$ (likewise for a_3). The eighth-order behavior is observed in the intensity of the field,

$$I(u) = |F(u)|^2 \propto a_2^8/(4!)^2. \quad (7)$$

At this point we have verified the result of KCG05 that the new mask designs allow light to leak as the eighth order of tip-tilt aberration (pointing error).

To see leakage for Zernike terms $j = 4$–10, we require terms with $l \geq 2$ in equation (6) and we find that *the intensity of the leakage varies as the fourth power of the aberration amplitude*. This behavior has been verified through our computer simulation described below.

For spherical aberration ($j = 11$), $l = 1$ results in constant illumination of the pupil and intensity leakage proportional to the square of the aberration amplitude. A higher order mask (e.g., twelfth-order mask consisting of three balanced quadratic terms; J. Crepp 2004, private communication) is required to further reject leakage caused by spherical aberration and higher order Zernike aberrations with quartic or higher order radial dependence. The additional aberration rejection comes at the expense of reduced throughput in the mask and Lyot stop.

[1] Amplitude variations $\delta a \ll 1$ can be treated in the same way by expanding the pupil function in a Taylor series, $P(u) = 1 + a(u) + a^2(u)\ldots$.

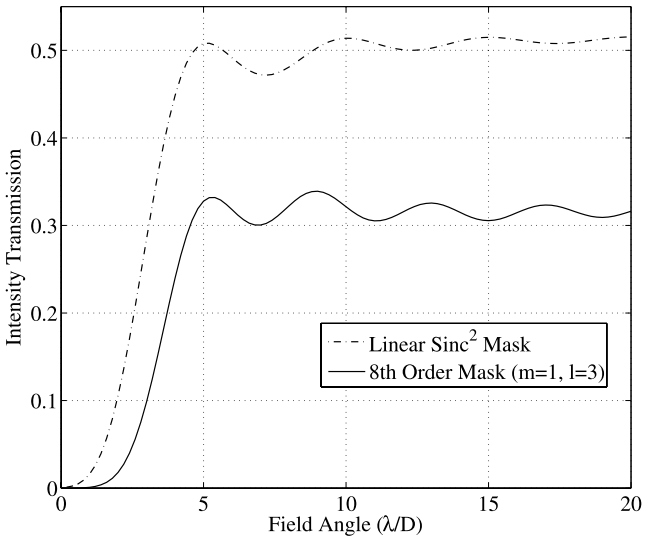

FIG. 1.—Intensity transmission including Lyot aperture throughput of a linear sinc^2 mask and a linear eighth-order mask with $m = 1$, $l = 3$ (see KCG05). The sinc^2 mask is optimized to have maximum throughput at $4\lambda/D$. The plots include averaging over the FWHM of the far-field image pattern.

3. COMPUTER SIMULATION

We model coronagraph performance with the assumption that the pupil, mask, Lyot, and final image planes are related by Fourier transforms (i.e., an ideal imaging system). Our model thus consists of two-dimensional array representations of an ideal pupil with uniform amplitude transmission, an ideal coronagraph mask that is opaque at the origin, a uniform hard-edge Lyot stop that transmits no light outside a specified aperture, and an ideal image plane. Adequate sampling (typically 1273×1273 arrays with 255×111 pupils) ensures that the noise floor in the ideal case is well below 1×10^{-10} of the peak stellar flux obtained if the coronagraph mask is omitted. The pupil considered was an unobscured 8×3.5 m ellipse, and the wavelength used was $\lambda = 550$ nm.

Aberrations described by Noll-ordered Zernike functions are introduced one by one in the pupil. Light scattered past the mask and Lyot stop is measured at the image plane where the "contrast" is computed. Contrast at a given point is defined as the average scattered light level inside a region A centered at that point, divided by the mask throughput at that point, and divided by the light level one would have if the image of a star were centered at that point in the absence of the coronagraph mask (Green & Shaklan 2003). The region A is defined as that inside the FWHM of the far-field image, which is given by the squared modulus of the Fourier transform of the Lyot aperture.

To compare the aberration sensitivity of the eighth-order mask to that of a fourth-order mask, we have chosen to maximize the combined mask and Lyot-stop throughput at $4\lambda/D$, the inner working angle for *TPF-C*. (We have slightly detuned the eighth-order mask from this condition, as explained below.) In Figure 1 we compare the throughputs for two designs: a linear $1 - \mathrm{sinc}^2$ mask and a linear eighth-order mask consisting of two balanced sinc functions parameterized by $m = 1$ and $l = 3$ (see KCG05 for further details). Note that for both masks, the maximum throughput at $4\lambda/D$ occurs when the mask's central lobe partially obscures light at this position; the mask throughput

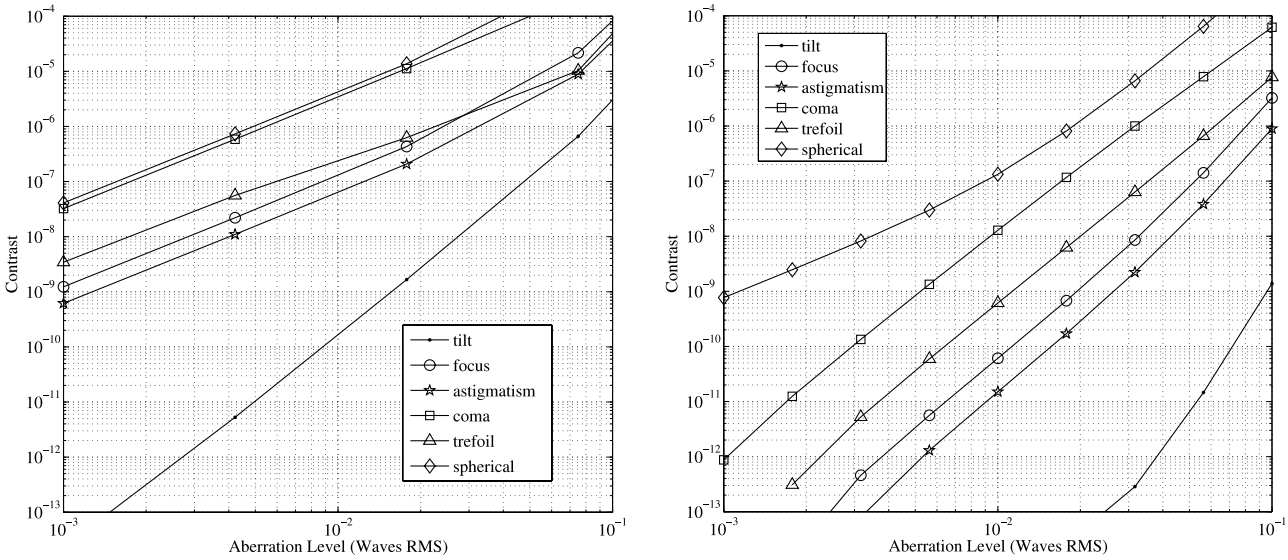

FIG. 2.—Aberration sensitivity of linear sinc^2 mask (*left*) and linear eighth-order mask (*right*) for low-order Zernike modes. For astigmatism, coma, and trefoil we display the more sensitive of the two orthogonal modes.

loss is balanced by the correspondingly larger Lyot stop available for the broader masks.

The eighth-order mask is one of a family of masks that trades inner working angle, ringing, and throughput. The particular choice ($m = 1$, $l = 3$) appears to be a reasonable compromise for these parameters, but other combinations may prove to have better overall performance than our first choice. To improve overall throughput at field angles $>4\lambda/D$, we have slightly compromised throughput of the eighth-order mask at $4\lambda/D$, from a maximum of 25% down to 24%, by broadening the mask, which in turn permits a wider Lyot stop. The $1 - \mathrm{sinc}^2$ mask and Lyot stop have 45% throughput at $4\lambda/D$.

The aberration sensitivity for the two masks is shown in Figure 2, where we plot the image-plane contrast at $4\lambda/D$ for Zernike modes 2–11. The eighth-order mask demonstrates (1) eighth-order sensitivity to wave front tilt; (2) fourth-order dependence on focus, astigmatism, coma, and trefoil; and (3) quadratic dependence on higher order Zernike modes, including spherical aberration. We note that the change in slope at contrast levels approaching 1×10^{-13} is due to the numerical noise floor of our simulation. We also point out that at large aberration levels (approaching 0.1 wave rms) high-order terms in the wave front expansion begin to dominate, resulting in slope changes.

The absence of second-order terms renders the eighth-order mask much less sensitive to aberrations than the linear sinc^2 mask. Table 1 gives the allowable change in rms wave front to maintain contrast at $4\lambda/D$ below 1×10^{-12} for individual aberrations. The new masks reduce tilt sensitivity by a factor of $\sim$16 at a contrast of 1×10^{-12} (the approximate *TPF* requirement for pointing errors). We also note that focus sensitivity, which drives many of the thermal and dynamic requirements in *TPF-C*, is reduced by more than *2 orders* of magnitude.

TABLE 1
ALLOWED ROOT MEAN SQUARE WAVE FRONT FOR CONTRAST = 1×10^{-12} AT $4\lambda/D$

Aberration	Eighth Order	Fourth Order	Relaxation Ratio
Tilt	4.3E−2	2.7E−3	16
Focus	3.8E−3	2.9E−5	132
Astigmatism	5.3E−3	4.0E−5	132
Coma	1.0E−3	5.6E−6	185
Trefoil	2.3E−3	1.7E−5	132
Spherical	3.5E−5	4.9E−6	7.2

NOTE.—Aberration units are waves rms at 550 nm.

4. ADVANTAGES FOR *TPF-C*

TPF-C has an aggressive coronagraph designed to work at $4\lambda/D$. In such close proximity to the core of the Airy function, small changes in low-order aberration content scatter significant levels of light (Green & Shaklan 2003). This in turn leads to optical surface figure stability requirements and structural dimensional stability requirements well beyond the current state of the art.

KCG05 invented eighth-order masks to relax the stringent pointing requirements associated with fourth-order masks. They suggested that the masks also reduce the leakage of light caused by higher order aberrations, a fact quantified in this paper. The advantages for the *TPF-C* design are clear: every term in the dynamic (thermal and jitter) portion of the error budget is substantially relaxed when fourth-order masks are replaced by eighth-order masks, even after accounting for the reduced throughput and lower resolution of the smaller Lyot stop. The impact is felt system-wide, as the requirements drive mass, jitter isolation, damping, materials choices, thermal isolation and control, etc.

A further advantage is that the masks help relax polarization leakage related to the angle of incidence of light across the off-axis *TPF-C* apertures (Elias et al. 2004; Breckinridge & Oppenheimer 2004). Unpolarized light incident on the telescope aperture becomes partially polarized; the state of polarization is aperture dependent with the most bothersome terms appearing as differential tilt, focus, and astigmatism between output polarization states. With fourth-order masks the issue is significant at the 1×10^{-9} contrast level. Eighth-order masks reduce the problem to an acceptable level $<1 \times 10^{-10}$.

5. CONCLUSION

We have quantified the way in which band-limited coronagraph masks filter aberrations. The derivative of the mask transmission function at the center of the mask determines the coefficient of sensitivity. We have shown that eighth-order

TABLE 2
First 15 Noll-ordered Zernike Polynomials

Mode	Name	Polynomial
Z1	Piston	1
Z2	Tip	$\sqrt{4}\rho\cos A$
Z3	Tilt	$\sqrt{4}\rho\sin A$
Z4	Focus	$\sqrt{3}(2\rho^2 - 1)$
Z5	Astigmatism	$\sqrt{6}\rho^2\sin 2A$
Z6	Astigmatism	$\sqrt{6}\rho^2\cos 2A$
Z7	Coma	$\sqrt{8}(3\rho^3 - 2\rho)\sin A$
Z8	Coma	$\sqrt{8}(3\rho^3 - 2\rho)\cos A$
Z9	Trefoil	$\sqrt{8}\rho^3\sin 3A$
Z10	Trefoil	$\sqrt{8}\rho^3\cos 3A$
Z11	Spherical	$\sqrt{5}(6\rho^4 - 6\rho^2 + 1)$
Z12	Second astigmatism	$\sqrt{10}(4\rho^4 - 3\rho^2)\cos 2A$
Z13	Second astigmatism	$\sqrt{10}(4\rho^4 - 3\rho^2)\sin 2A$
Z14	Tetrafoil	$\sqrt{10}\rho^4\cos 4A$
Z15	Tetrafoil	$\sqrt{10}\rho^4\sin 4A$

masks greatly reduce sensitivity to focus, coma, astigmatism, and trefoil and provide some relief for spherical aberration as well. The masks lead to a significant relaxation of key elements of the *TPF-C* error budget.

The next step in adopting the new masks for *TPF-C* is to tolerance the mask manufacturing errors. We are considering multiple tolerancing criteria, including the sensitivity of the mask to changes in low-order aberration content as well as the static leakage caused by mask imperfections (e.g., phase transmission errors and transmission of orthogonal states of polarization). The tolerancing will account for the ability of a deformable mirror in the system to mitigate some leakage across a finite bandwidth.

We thank Marc Kuchner for his helpful comments and Oliver Lay for his critical reading of this paper. This work was performed at the Jet Propulsion Laboratory, California Institute of Technology, under contract to the National Aeronautics and Space Administration.

APPENDIX

ZERNIKE POLYNOMIAL TABLE

Table 2 lists the first 15 Noll-ordered Zernike polynomials (Noll 1976). For our modeling of the elliptical *TPF-C* aperture (semimajor axis $r_1 = 4$ m, semiminor axis $r_2 = 1.75$ m), the Zernike modes are matched to the aperture by replacing radial coordinate $\rho^2 = x^2 + y^2$ with $\rho^2 = (x/r_1)^2 + (y/r_2)^2$. This does not affect the orthogonality of the modes. It does, however, change the physical interpretation of the modes because the curvature is different in x and y.

REFERENCES

Breckinridge, J. B., & Oppenheimer, B. R. 2004, ApJ, 600, 1091
Debes, J. H., Ge, J., Kuchner, M. J., & Rogosky, M. 2004, ApJ, 608, 1095
Elias, N. M., Bates, R., & Turner-Valle, J. 2004, Proc. SPIE, 5555, 248
Ford, V. G., et al. 2004, Proc. SPIE, 5487, 1274
Gaskill, J. D. 1978, Linear Systems, Fourier Tranforms, and Optics (New York: Wiley)
Green, J. J., & Shaklan, S. B. 2003, Proc. SPIE, 5170, 25
Green, J. J., Shaklan, S. B., Kasdin, N. J., & Vanderbei, R. J. 2004, Proc. SPIE, 5487, 1358
Guyon, O. 2003, A&A, 404, 379
Kasdin, N. J., Vanderbei, R. J., Spergel, D. N., & Littman, M. G. 2003, ApJ, 582, 1147
Kuchner, M. J., Crepp, J., & Ge, J. 2005, ApJ, in press (KCG05)
Kuchner, M. J., & Spergel, D. N. 2003, ApJ, 594, 617
Kuchner, M. J., & Traub, W. A. 2002, ApJ, 570, 900
Noll, R. J. 1976, J. Opt. Soc. Am., 66, 207
Rouan, D., Boccaletti, A., Riaud, P., & Baudrand, J. 2003, Proc. SPIE, 4860, 192
Shao, M., Wallace, J. K., Levine, B. M., & Liu, D. T. 2004, Proc. SPIE, 5487, 1296
Trauger, J. T., et al. 2004, Proc. SPIE, 5487, 1330
Woolf, N. J., & Angel, J. R. P. 1997, in ASP Conf. Ser. 119, Planets Beyond the Solar System and the Next Generation of Space Missions, ed. D. Soderblom (San Francisco: ASP), 285